

DOI: 10.1002/ange.200502291

# Assembly of Dendrimers with Redox-Active $[\text{CpFe}(\mu_3\text{-CO})_4]$ Clusters at the Periphery and Their Application to Oxo-Anion and Adenosine-5'-Triphosphate Sensing\*\*

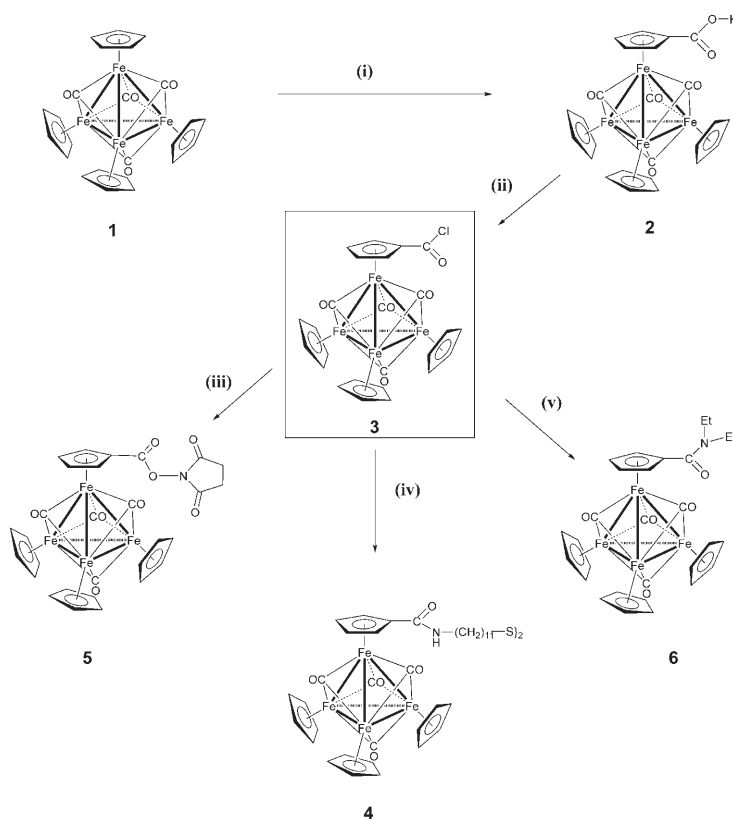
Jaime Ruiz Aranzaes, Colette Belin, and Didier Astruc\*

Metallodendrimers<sup>[1–8]</sup> are well-established nanomaterials that have applications as electronic devices,<sup>[2]</sup> sensors,<sup>[3]</sup> and catalysts.<sup>[3,4]</sup> However, only a few examples are known with transition-metal clusters at the dendrimer periphery.<sup>[5]</sup> A star decorated with four polyoxometallate groups active in oxidation catalysis was reported,<sup>[6]</sup> and other redox-active transition-metal groups surrounding dendrimers at the periphery include metallocenes<sup>[7]</sup> and ruthenium polypyridine complexes.<sup>[2a]</sup> These molecular assemblies show promise as electronic devices and sensors which can be used by electrode modification.<sup>[8]</sup> Herein we report 1) functionalization of the long-known tetrairon cluster  $[\text{CpFe}(\mu_3\text{-CO})_4]$  (**1**),<sup>[9,10]</sup> the prototype of redox-rich organometallic clusters; 2) derivatization of 9-, 16-, and 27-branched dendrimers therewith; 3) redox behavior and redox robustness of these new metallodendrimers and formation of modified electrodes on which the cluster dendrimers are more strongly adsorbed with increasing size; 4) their application as selective sensors for oxo anions including adenosine-5'-triphosphate ( $\text{ATP}^{2-}$ ); and 5) dendritic and structural effects on anion recognition, in particular the selectivity of recognition of  $\text{ATP}^{2-}$  in the presence of other anions and, for the first time, better recognition of  $\text{ATP}^{2-}$  than  $\text{H}_2\text{PO}_4^-$ .

Cluster **1** and its rich redox chemistry have been known for a long time.<sup>[9]</sup> We have synthesized its acyl chloride derivative **3** by reaction of the acid  $[\text{Fe}_4\text{Cp}_3(\eta^5\text{-C}_5\text{H}_4\text{CO}_2\text{H})]$  (**2**)<sup>[9d]</sup> with  $(\text{COCl})_2$ , the disulfide **4** by reaction of **3** with

$[-\text{S}(\text{CH}_2)_{11}\text{NH}_3^+\text{Cl}^-]_2$ , and the *N*-succinimidyl ester **5** by reaction of **3** with *N*-hydroxysuccinimide (Scheme 1).

Complex **3** reacts with 9-branched amino dendrimer **7** in the presence of  $\text{NEt}_3$  to give the expected 9-branched amido cluster dendrimer **8** [Eq. (1)]. However, this is not the case for commercial (DSM) third-generation 16-branched amino dendrimer **9**,<sup>[11]</sup> probably for steric reasons. Compound **9** did not give the expected dendritic amide complex in the presence of  $\text{NEt}_3$ , but unexpected formation of the diethyl-amido cluster **6** was observed, presumably resulting from electron transfer from  $\text{NEt}_3$  to **3** to generate the acyl radical



**Scheme 1.** i) a)  $\text{LiN}(\text{Pr})_2$ ,  $-40^\circ\text{C}$ , 1 h, THF; b)  $\text{CO}_2$ ,  $-40 \rightarrow 20^\circ\text{C}$ ; c) aq. 1 N HCl,  $20^\circ\text{C}$  (30% yield); ii)  $(\text{COCl})_2$ ,  $\text{CH}_2\text{Cl}_2$ ,  $0^\circ\text{C}$ , 12 h (100% yield); iii) *N*-hydroxysuccinimide,  $\text{NEt}_3$ ,  $\text{CH}_2\text{Cl}_2$ ,  $20^\circ\text{C}$ , 12 h (85% yield); iv)  $[-\text{SCH}_2]_{11}\text{NH}_3^+\text{Cl}^-$ ,  $\text{NEt}_3$ ,  $\text{CH}_2\text{Cl}_2$ ,  $20^\circ\text{C}$ , 12 h (63% yield); v)  $\text{NEt}_3$ ,  $\text{CH}_2\text{Cl}_2$ ,  $20^\circ\text{C}$ , 12 h (65% yield).

$[\text{Fe}_4(\mu_3\text{-CO})_4\text{Cp}_3(\eta^5\text{-C}_5\text{H}_4\text{CO}^\bullet)]$ , which further reacts with  $\text{NEt}_3^+$  or  $\text{NEt}_2^\bullet$ . Successful functionalization of dendrimer **9** was performed by using *N*-succinimidyl ester **5**<sup>[12]</sup> to give 16-branched amido cluster dendrimer **10** [Eq. (2)].

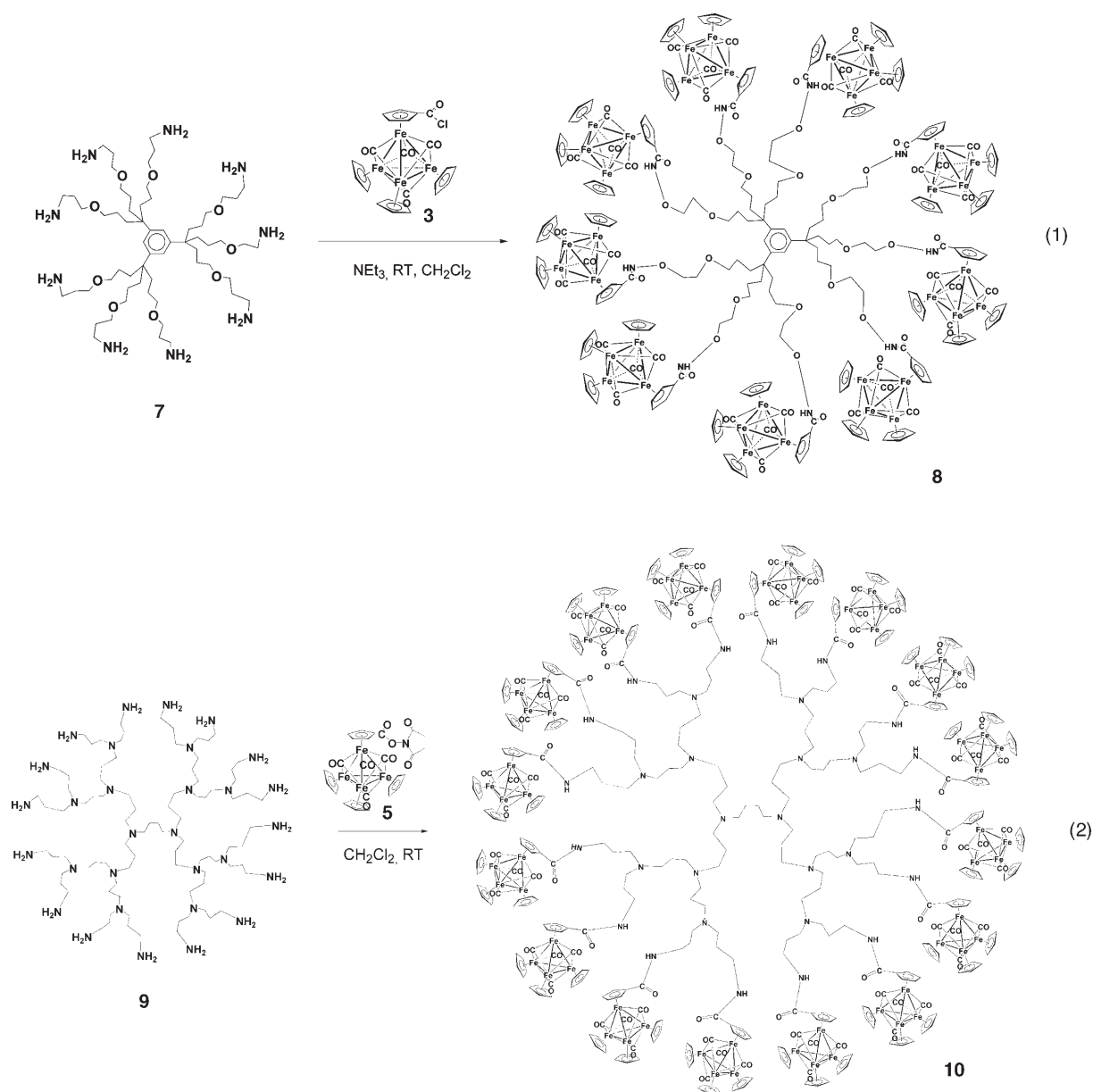
The reaction of **5** with the fourth-generation 32-branched amino dendrimer (DSM, following that of third-generation **9**) gave a dark green powder that was insoluble in all solvents, obviously due to excess steric bulk at the dendrimer periphery. However, the functionalization reaction worked smoothly with the new 27- $\text{NH}_2$  dendrimer **11**<sup>[13]</sup> to give 27- $\text{Fe}_4$  dendrimer **12** [Eq. (3)], because the interior and peripheral tethers are longer in **11** than in the diaminobutane dendrimers from DSM. The new metallodendrimers **8**, **10**, and **12** are air-stable, forest-green powders. They were characterized by

[\*] Dr. J. R. Aranzaes, Prof. D. Astruc  
Nanosciences and Catalysis Group  
LCOO, UMR CNRS No 5802  
Université Bordeaux I  
33405 Talence Cedex (France)  
Fax: (+33) 540-006-646  
E-mail: d.astruc@lcoo.u-bordeaux1.fr

Dr. C. Belin  
LPCM, UMR CNRS No 5803  
Université Bordeaux I  
33405 Talence Cedex (France)

[\*\*] Financial support from the Institut Universitaire de France (IUF, DA), the Université Bordeaux I, and the CNRS is gratefully acknowledged.

Supporting information for this article is available on the WWW under <http://www.angewandte.org> or from the author.



standard spectroscopic and elemental analyses, and atomic force microscopy (AFM) on **10** and **12** (Figure 1 and Supporting Information) showed monolayers of aggregated metallodendrimers are formed on the mica surface. Indeed, the heights of 1.5 nm for **10** and 2.4 nm for **12** are reproducibly obtained by AFM and correspond to the dimensions of slightly flattened molecular models.<sup>[14]</sup>

The cyclovoltammograms (CVs) of dendrimer clusters **8**, **10**, and **12** in  $\text{CH}_2\text{Cl}_2$  (Pt, 0.1 M  $n\text{Bu}_4\text{NPF}_6$ ) resemble that of the monomeric cluster **1**,<sup>[9c]</sup> that is, the clusters are sufficiently remote from one another in the dendrimers to render the electrostatic factor almost nil. Therefore all the redox sites corresponding to the redox change  $\text{Fe}_4 \rightarrow \text{Fe}_4^+$  appear in a single reversible wave (the other waves  $\text{Fe}_4^+ \rightarrow \text{Fe}_4^{2+}$  and  $\text{Fe}_4^0 \rightarrow \text{Fe}_4^-$  are also reversible, see Supporting Information).<sup>[15]</sup> For this wave, the Bard–Anson equation<sup>[15a]</sup> was applied to determine the number of electrons under con-

ditions that avoid adsorption. This gave a result of  $27 \pm 3$  electrons in  $\text{CH}_2\text{Cl}_2$  and DMF with  $[\text{FeCp}^*_2]$  ( $\text{Cp}^* = \eta^5\text{-C}_5\text{Me}_5$ ) as internal reference. This stoichiometry could be confirmed by titration of **12** in  $\text{CH}_2\text{Cl}_2$  with 27 equiv of green  $[\text{CpFe}(\eta^5\text{-C}_5\text{H}_4\text{COCH}_3)]\text{PF}_6$ , which generates  $[\text{CpFe}(\eta^5\text{-C}_5\text{H}_4\text{COCH}_3)]$  and a dark green precipitate of  $[\text{12}](\text{PF}_6)_{27}$ , characterized by the CO IR band at  $\tilde{\nu}_{\text{CO}} = 1690 \text{ cm}^{-1}$ , 55  $\text{cm}^{-1}$  higher than  $\tilde{\nu}_{\text{CO}}$  of **12** ( $1635 \text{ cm}^{-1}$ ). The color of the  $\text{CH}_2\text{Cl}_2$  solution changes from dark green (**12**) to red (acetylferrocene) at the equivalence point.<sup>[9]</sup>

This property offers the possibility of recognizing anions, an area pioneered and deeply studied by Beer et al.,<sup>[16]</sup> then also by Moutet et al.,<sup>[17]</sup> with endoreceptors functionalized with various redox active species, although clusters have not yet been used for such sensing. We are dealing here with dendritic exoreceptors, a family that also proved successful for sensing, but only with metallocene units.<sup>[3b]</sup>

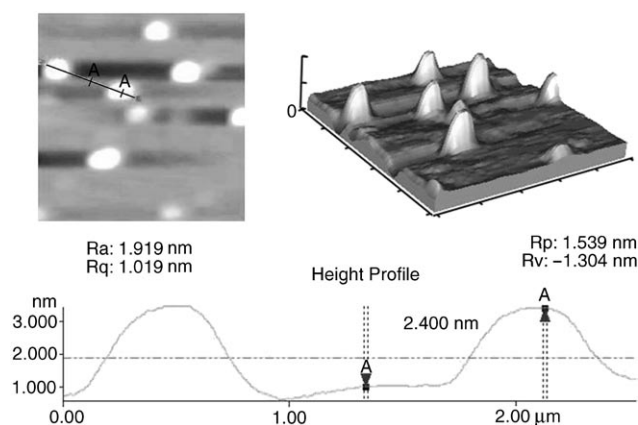
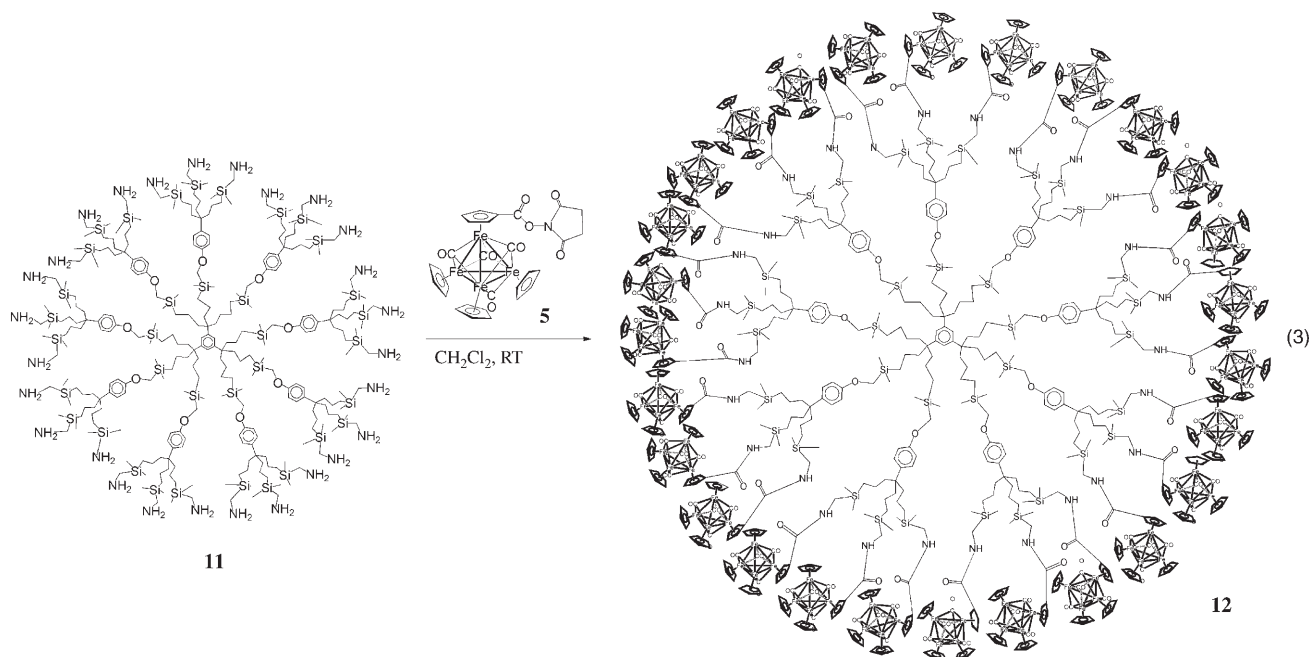


**Figure 1.** AFM pictures of 27-Fe<sub>4</sub> cluster dendrimer **12** on a mica surface.

Recognition of the oxo anions HSO<sub>4</sub><sup>-</sup>, H<sub>2</sub>PO<sub>4</sub><sup>-</sup>, and adenosine-5'-triphosphate (ATP<sup>2-</sup>) as their *n*-tetrabutylammonium salts by exoreceptors **8**, **10**, and **12** was investigated by adding their *n*Bu<sub>4</sub>N<sup>+</sup> salts to electrochemical cells containing a solution of the exoreceptor in CH<sub>2</sub>Cl<sub>2</sub> at a Pt anode. Interestingly, for comparison, addition of these salts to a solution of the monomeric amido cluster **6** or [Fe<sub>4</sub>(CO)<sub>4</sub>Cp<sub>3</sub>(C<sub>5</sub>H<sub>4</sub>CONH*n*Pr)] did not provoke any change in the CV of the monomeric cluster. On the other hand, addition of (*n*Bu<sub>4</sub>N)<sub>2</sub>(ATP) to one of these three dendritic clusters (even in the presence of HSO<sub>4</sub><sup>-</sup> and Cl<sup>-</sup>, vide infra) gave recognition features that were very different from one another and different from those of previous dendritic metallocenyl exoreceptors.<sup>[3b]</sup>

With H<sub>2</sub>PO<sub>4</sub><sup>-</sup>, a progressive wave shift was observed on titration, which was approximated according to the weak-interaction case in the Echegoyen–Kaifer model,<sup>[18]</sup> and the

value of the apparent association constant was  $K_{(+)}$  = 412 ± 70 (Supporting Information).

Contrary to the case of (*n*Bu<sub>4</sub>N)H<sub>2</sub>PO<sub>4</sub>, addition of (*n*Bu<sub>4</sub>N)<sub>2</sub>(ATP) to the electrochemical cell containing the solution of the host in CH<sub>2</sub>Cl<sub>2</sub> provoked the appearance of a new CV wave, although with very different features for each dendrimer. In addition, the potential shifts are larger than those observed with (*n*Bu<sub>4</sub>N)H<sub>2</sub>PO<sub>4</sub> (Figure 2, Table 1), which contrasts with the behavior found for all metallocenyl dendrimers. The titration diagrams were recorded by using the decrease in intensity of the initial wave and increase in intensity of the new wave for both **10** and **12**. They show equivalence points for 0.5–0.6 equiv (*n*Bu<sub>4</sub>N)<sub>2</sub>(ATP) per branch due to the double negative charges, which seemingly means that each phosphate monoanion unit of ATP<sup>2-</sup> interacts with one Fe<sub>4</sub> cluster branch. Various other stoichiometries have been reported in such titrations.<sup>[17]</sup>

The addition of (*n*Bu<sub>4</sub>N)HSO<sub>4</sub> to dendrimer **10** provokes a shift of the initial wave. This shift reaches 110 mV at saturation, which leads to an apparent association constant of  $K_{+}$  = (55 ± 5) × 10<sup>3</sup> L mol<sup>-1</sup>. The titration diagram shows an equivalence point at 0.75 equiv (*n*Bu<sub>4</sub>N)HSO<sub>4</sub> per Fe<sub>4</sub> cluster branch, although saturation is obtained at 1 equiv (*n*Bu<sub>4</sub>N)HSO<sub>4</sub> per branch (see Supporting Information). In this case the interaction is of the weak type, loose, and not selective.

The addition of equimolar amounts of (*n*Bu<sub>4</sub>N)<sub>2</sub>(ATP), (*n*Bu<sub>4</sub>N)HSO<sub>4</sub>, and (*n*Bu<sub>4</sub>N)Cl to the electrochemical cell containing dendrimer **10** leads to a shift of the initial wave by 0.1 V. The equivalence point is reached at 0.7 equiv (*n*Bu<sub>4</sub>N)<sub>2</sub>(ATP) (see Supporting Information), although no new CV wave is observed. This wave shift instead of the appearance of a new wave, when only (*n*Bu<sub>4</sub>N)<sub>2</sub>(ATP) is added, and the slight increase in stoichiometry, can tentatively be taken into account by a dynamic equilibrium among the various ions of

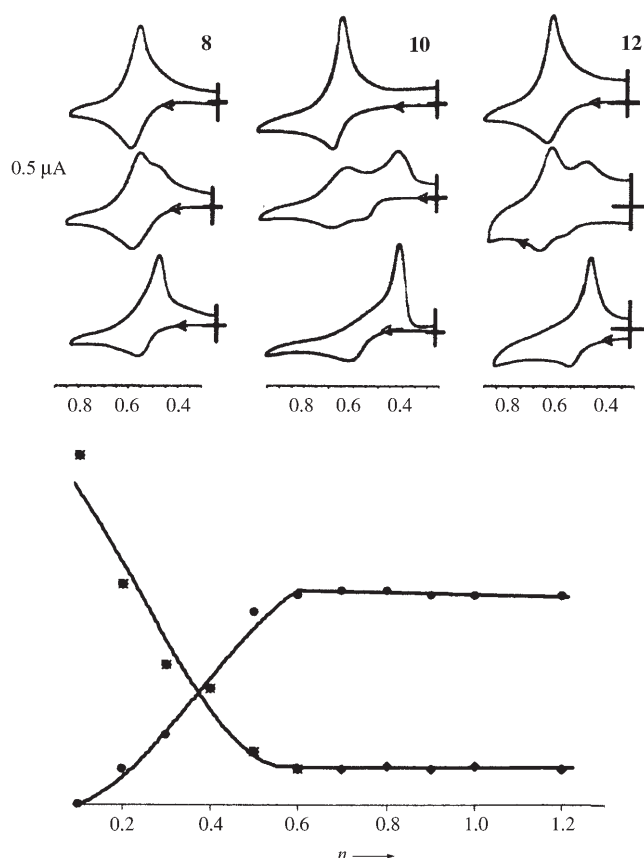


**Figure 2.** Titration of  $\text{ATP}^{2-}$  with **8**, **10**, and **12** ( $6 \times 10^{-5} \text{ M}$ ) in  $\text{CH}_2\text{Cl}_2$ . Top: CVs before (bottom), during (middle), and after (top) addition of  $(n\text{Bu}_4\text{N})_2(\text{ATP})$  (x axis: voltage [V] vs  $[\text{FeCp}^*_2]$ ). Bottom: Decrease of the intensity of the initial CV wave (■) and increase of the intensity of the new CV wave (●) versus the number  $n$  of equivalents of  $(n\text{Bu}_4\text{N})_2(\text{ATP})$  added per cluster branch of **10**.

**Table 1:** Cyclic voltammetry data for **8**, **12** and **10** before, during, and after titration of  $(n\text{Bu}_4\text{N})_2(\text{ATP})$ .

	$E_{1/2}^{[a]}$ ( $E_{\text{pa}} - E_{\text{pc}}$ )	$E_{1/2 \text{ free}} - E_{1/2 \text{ new}}^{[b]}$	$E_{1/2 \text{ bound}}^{[c]}$ ( $E_{\text{pa}} - E_{\text{pc}}$ )	$K_+/K_0^{[d]}$
monomer	0.630 (60)		0.610 (100)	
<b>8</b>	0.580 (30)	0.040	0.465 (100)	5
<b>12</b>	0.620 (30)	0.110	0.500 (100)	
<b>10</b>	0.590 (30)	0.165	0.385 (200)	700
modified Pt electrode with <b>12</b>	0.600 (10)	0.095	0.495 (70)	43
modified Pt electrode with <b>10</b>	0.590 (30)	0.070	0.500 (100)	16

[a]  $E_{1/2}$  [V] vs  $[\text{FeCp}^*_2]$  (internal reference) convertible into the value vs  $[\text{FeCp}_2]$  by subtracting 0.545 V;<sup>[19]</sup> electrolyte,  $(n\text{Bu}_4\text{N})\text{PF}_6$ ; working and counterelectrodes, Pt; solvent,  $\text{CH}_2\text{Cl}_2$ . The  $E_{\text{pa}} - E_{\text{pc}}$  values are indicated in parentheses. [b] Difference of  $E_{1/2}$  value [V] between the free wave and the new wave at half titration in order to observe and compare both waves (see Figure 1). [c]  $E_{1/2}$  after addition of 0.5–0.6 equiv  $\text{ATP}^{2-}$  (equivalence point). [d] Ratio between the apparent association constants of the cationic ( $K_+$ ) and neutral form ( $K_0$ ) with  $\text{ATP}^{2-}$ .

the ion pairs and complexation kinetics that are different in the presence and absence of a mixture of anions.

Modification of a Pt electrode with dendrimers<sup>[6,7]</sup> such as **10** and **12** is possible (although not cleanly with the mono-cluster thiol derivative **4**); the best results were obtained with **12** due to its larger size ( $E_{\text{pa}} - E_{\text{pc}} = 10 \text{ mV}$ , see Supporting Information). Recognition of  $\text{ATP}^{2-}$  also then proceeds with the replacement of the initial wave by the new wave at less

positive potential. After disappearance of the initial wave, the final chemically reversible wave has an  $E_{\text{pa}} - E_{\text{pc}}$  value of 70 or 100 mV (Table 1), which signifies that electron transfer at the electrode surface is slow. This is due to structural reorganization of the dendritic host–guest supramolecular assembly that involves, as in solution, formation versus disruption of large ion pairs in synergy with double hydrogen bonding between the oxo anion and the amido group.<sup>[16]</sup> The shape of this wave is a fingerprint of the oxo anion. The salt  $(n\text{Bu}_4\text{N})_2(\text{ATP})$  can be washed away with  $\text{CH}_2\text{Cl}_2$  to leave the modified electrode, which now only shows the initial wave of the dendritic cluster, although its current intensity is lower than initially. Subsequently, this washed, modified electrode can be used again.

The addition of equimolar amounts of  $(n\text{Bu}_4\text{N})_2(\text{ATP})$ ,  $(n\text{Bu}_4\text{N})\text{HSO}_4$ , and  $(n\text{Bu}_4\text{N})\text{Cl}$  to the electrochemical cell containing dendrimer **12** leads to the appearance of a new wave, but the initial wave does not completely disappear after equivalence, consistent with the suggested hypothesis of a dynamic equilibrium (see below and Supporting Information).

In conclusion, we have successfully functionalized the cluster  $[\text{CpFe}(\mu_3\text{-CO})]_4$  for covalent attachment through a Cp ligand to the periphery of 9-, 16-, and 27-branched dendrimers and characterized the resulting cluster dendrimers inter alia by AFM on mica, which showed their flattening. Their cyclic voltammograms show a single reversible wave for the redox change  $\text{Fe}_4 \rightarrow \text{Fe}_4^+$ , and this CV wave can be used for redox recognition and titration of oxo anions and in particular  $(n\text{Bu}_4\text{N})_2(\text{ATP})$  in  $\text{CH}_2\text{Cl}_2$  solution. The larger cathodic wave shift with **10** than with **12** on  $\text{ATP}^{2-}$  addition is presumably due to the shorter distance between two clusters in **10** (12 bonds) than in **12** (16 bonds). Remarkably, and for the first time,  $(n\text{Bu}_4\text{N})_2(\text{ATP})$  is better recognized than

$(n\text{Bu}_4\text{N})\text{H}_2\text{PO}_4$ , whereas the opposite holds with metallocenyl dendrimers. This specificity is certainly due to the mutual nanosize of the  $\text{Fe}_4$  clusters and  $\text{ATP}^{2-}$ , which facilitates their interaction, whereas the smaller ferrocenyl groups do not exhibit this property. Dendritic effects (dendritic structure and compacity) are dramatic as is the replacement of metallocenes for cluster redox sensors. A Pt electrode modified with the 16- $\text{Fe}_4$  or 27- $\text{Fe}_4$  dendrimer provides selective ATP recognition. It is possible to wash the dendrimer with  $\text{CH}_2\text{Cl}_2$  for recycling, and the quality of the modified electrode is optimum

with the larger 27- $\text{Fe}_4$  dendrimer **12** due to better adsorption. Finally, given the known properties of **1** as a selective hydrogenation catalyst for various functional groups,<sup>[9h]</sup> this family of metallodendritic catalysts should also find use as recyclable catalysts.<sup>[4,20]</sup>



## Experimental Section

27-cluster dendrimer **12**: The 27-NH<sub>2</sub> dendrimer **11** (0.020 g,  $3.8 \times 10^{-3}$  mmol) and triethylamine (0.029 mL, 0.2 mmol) were dissolved in dry CH<sub>2</sub>Cl<sub>2</sub>. Complex **5** (0.112 g, 0.152 mmol) in CH<sub>2</sub>Cl<sub>2</sub> (10 mL) was added to this solution. The green solution was stirred at room temperature for 7 d under positive nitrogen pressure. The solution was then washed twice with a saturated sodium carbonate solution and twice with water, and the green organic solution was dried over sodium sulfate. The volume was reduced to 5 mL, and 25 mL of dry diethyl ether was added, which gave a green powder. This precipitate was dissolved in 5 mL of CH<sub>2</sub>Cl<sub>2</sub>, and the solution was poured over 25 mL of dry diethyl ether with stirring, which yielded a forest-green precipitate. The powdery 27-Fe<sub>4</sub> dendrimer **12** was finally dried under vacuum (0.030 g, 30% yield); dendrimer **10** was synthesized in the same way (see data in Supporting Information).

See the Supporting Information for the syntheses of all the clusters and dendrimers, AFM, and CVs including redox recognition and titration data.

Received: June 30, 2005

Revised: September 28, 2005

Published online: November 22, 2005

**Keywords:** anions · cluster compounds · dendrimers · iron · sensors

- [1] Books on dendrimers: a) G. R. Newkome, C. N. Moorefield, F. Vögtle, *Dendrimers and Dendrons: Concepts, Synthesis, Applications*, Wiley-VCH, Weinheim, **2001**; b) *Dendrimers and Other Dendritic Polymers* (Eds.: J. M. J. Fréchet, D. A. Tomalia), Wiley, New York, **2002**; c) *Dendrimers and Nanosciences*, Vol. 6 (issues 8–10: Guest Ed.: D. Astruc), Elsevier, Paris, **2003**.
- [2] Reviews on metal dendrimers: a) V. Balzani, S. Campana, G. Denti, A. Juris, S. Serroni, M. Venturi, *Acc. Chem. Res.* **1998**, *31*, 26; b) G. R. Newkome, C. N. Moorefield, *Chem. Rev.* **1999**, *99*, 1689; c) M. A. Hershaw, J. R. Moss, *Chem. Commun.* **1999**, 1.
- [3] Metal dendritic sensors: a) M. Albrecht, N. J. Hovestad, J. Boersma, G. van Koten, *Chem. Eur. J.* **2001**, *7*, 1289; A. W. Kleij, A. Ford, J. T. B. H. Jastrzebski, G. van Koten in ref. [1b], p. 185; b) D. Astruc, M.-C. Daniel, J. Ruiz, *Chem. Commun.* **2004**, 2637; see also refs. [7, 8].
- [4] Metal dendritic catalysts: a) G. E. Oosterom, J. N. H. Reek, P. C. J. Kamer, P. W. N. M. van Leeuwen, *Angew. Chem.* **2001**, *113*, 1878; *Angew. Chem. Int. Ed.* **2001**, *40*, 1828; b) D. Astruc, F. Chardac, *Chem. Rev.* **2001**, *101*, 1991.
- [5] a) Dendrimers with clusters at the periphery: G. R. Newkome, C. N. Moorefield, *Polym. Prepr. Am. Chem. Soc. Div. Polym. Chem.* **1993**, *34*, 75; b) M. Ferrer, R. Reina, O. Rossell, M. Seco, *Coord. Chem. Rev.* **1999**, *193–195*, 619; c) E. Alonso, D. Astruc, *J. Am. Chem. Soc.* **2000**, *122*, 3222.
- [6] Dendrimers with redox-active clusters at the periphery: H. Zheng, G. R. Newkome, C. L. Hill, *Angew. Chem.* **2000**, *112*, 1841; *Angew. Chem. Int. Ed.* **2000**, *39*, 1772.
- [7] Reviews on ferrocenyl dendrimers and their redox activity: ref. [3b] and C. M. Casado, I. Cuadrado, M. Moran, B. Alonso, B. Garcia, B. Gonzales, J. Losada, *Coord. Chem. Rev.* **1999**, *185–186*, 53.
- [8] Dendritic redox-active assemblies modifying electrodes and their redox properties: refs. [3b, 7] and M. Yamada, I. Quieros, J. Mizutani, K. Kubo, I. Nishihara, *Phys. Chem. Chem. Phys.* **2001**, *3*, 3377; M. Yamada, H. Nishihara, *Chem. Commun.* **2002**, 2578.
- [9] a) R. B. King, *Inorg. Chem.* **1966**, *5*, 2227; b) T. Toan, W. P. Felhammer, L. F. Dahl, *J. Am. Chem. Soc.* **1972**, *94*, 3389; c) J. A. Ferguson, T. J. Meyer, *J. Am. Chem. Soc.* **1972**, *94*, 3409; d) A. J. White, A. J. Cunningham, *J. Chem. Educ.* **1980**, *57*, 317; e) M. D. Westmeyer, M. A. Massa, T. B. Rauchfuss, S. R. Wilson, *J. Am. Chem. Soc.* **1998**, *120*, 114; f) W.-Y. Yeh, C.-Y. Wu, L.-W. Chiou, *Organometallics* **1999**, *18*, 3547; g) J. Ruiz, F. Ogliaro, J.-Y. Saillard, J.-F. Halet, F. Varret, D. Astruc, *J. Am. Chem. Soc.* **1998**, *120*, 1163; h) E. Alonso, J. Ruiz, D. Astruc, *C. R. Acad. Sci. Ser. IIc* **2001**, *3*, 189; i) cluster **1** is also a selective hydrogenation catalyst: see for instance j) C. U. Pittman, R. C. Ryan, J. McGee, J. P. O'Connor, *J. Organomet. Chem.* **1979**, *178*, C43.
- [10] C. Valério, J.-L. Fillaut, J. Ruiz, J. Guittard, J.-C. Blais, D. Astruc, *J. Am. Chem. Soc.* **1997**, *119*, 2588.
- [11] E. M. M. de Brabander-van den Berg, E. W. Meijer, *Angew. Chem.* **1993**, *105*, 1370; *Angew. Chem. Int. Ed. Engl.* **1993**, *32*, 1308; for examples of seminal applications of diaminobutane-based polyamine dendrimers using an amido linkage, see: J. F. G. A. Jansen, E. M. M. de Brabander-van der Berg, E. W. Meijer, *Science* **1994**, *266*, 1226.
- [12] For previous syntheses of amides from *N*-succinimidyl esters, see: P. D. Beer, C. Harlewood, D. Hesk, J. Hodacova, S. E. Stokes, *J. Chem. Soc. Dalton Trans.* **1993**, 1327.
- [13] J. Ruiz, G. Lafuente, S. Marcen, C. Ornelas, S. Lazarre, E. Cloutet, J.-C. Blais, D. Astruc, *J. Am. Chem. Soc.* **2003**, *125*, 7250.
- [14] a) A. Hierlemann, J. K. Campbell, L. A. Baker, R. M. Crooks, A. J. Riccio, *J. Am. Chem. Soc.* **1998**, *120*, 5323; b) J. Li, L. T. Piehler, D. Qin, J. R. Baker, Jr., D. A. Tomalia, D. J. Meier, *Langmuir* **2000**, *16*, 5613.
- [15] a) J. B. Flanagan, S. Margel, A. J. Bard, F. C. Anson, *J. Am. Chem. Soc.* **1978**, *100*, 4248; b) A. J. Bard, R. L. Faulkner, *Electrochemical Methods*, Wiley, New York, **1980**.
- [16] P. D. Beer, *Adv. Inorg. Chem.* **1993**, *39*, 79; P. D. Beer, *Chem. Commun.* **1996**, 689 (feature article); P. D. Beer, *Acc. Chem. Res.* **1998**, *31*, 71; P. D. Beer, P. A. Gale, Z. Chen, *Adv. Phys. Org. Chem.* **1998**, *31*, 1; P. D. Beer, *Angew. Chem.* **2001**, *113*, 502; *Angew. Chem. Int. Ed.* **2001**, *40*, 486; J. H. R. Tucker, S. R. Collison, *Chem. Soc. Rev.* **2002**, *31*, 147; P. D. Beer, E. J. Hayes, *Coord. Chem. Rev.* **2003**, *240*, 167; W. W. H. Wong, D. Curiel, S.-W. Lai, M. G. B. Drew, P. D. Beer, *Dalton Trans.* **2005**, 774, and references therein.
- [17] O. Reynes, J.-C. Moutet, J. Pecaut, G. Royal, E. Saint-Aman, *Chem. Eur. J.* **2000**, *6*, 2544; O. Reynes, G. Royal, E. Chainet, J.-C. Moutet, E. Saint-Aman, *Electroanalysis* **2002**, *15*, 65; O. Reynes, T. Gulon, J.-C. Moutet, G. Royal, E. Saint-Aman, *J. Organomet. Chem.* **2002**, *656*, 116; O. Reynes, J.-C. Moutet, J. Pecaut, G. Royal, E. Saint-Aman, *New J. Chem.* **2002**, *26*, 9; C. Bucher, D. H. Devillers, J.-C. Moutet, G. Royal, E. Saint-Aman, *New J. Chem.* **2004**, *28*, 1584; O. Reynes, C. Bucher, J.-C. Moutet, G. Royal, E. Saint-Aman, E.-M. Ungureanu, *J. Electroanal. Chem.* **2005**, *580*, 291.
- [18] S. R. Miller, D. A. Gustowski, Z.-H. Chen, G. W. Gokel, L. Echegoyen, A. E. Kaifer, *Anal. Chem.* **1988**, *60*, 2021.
- [19] D. Astruc in *Electron Transfer in Chemistry*, Vol. 2 (Ed.: V. Balzani), Wiley-VCH, Weinheim, **2001**, Sec. 2, chap. 4, pp. 714–803.
- [20] We are grateful to a reviewer for useful remarks concerning the redox-recognition aspects.